ACS Catalysis

Research Article

pubs.acs.org/acscatalysis

Impact and Detailed Action of Sulfur in Syngas on Methane Synthesis on Ni/γ-Al_2O_3 Catalyst

Benoit Legras, Vitaly V. Ordomsky, Christophe Dujardin, Mirella Virginie, and Andreï Y. Khodakov*

Unité de Catalyse et de Chimie du Solide, UMR CNRS 8181, Université Lille 1-ENSCL-EC Lille, Cité Scientifique, Bâtiment C3, 59655 Villeneuve d'Ascq, France

Supporting Information

ABSTRACT: Stability and deactivation phenomena are of utmost importance for metal nanocatalysts from both fundamental and industrial points of view. The presence of small amounts of sulfur at ppm and ppb levels in the synthesis gas produced from fossil and renewable sources (e.g., biomass, coal) is a major reason for deactivation of nickel catalysts for carbon monoxide hydrogenation. This paper addresses reaction pathways and deactivation mechanisms of alumina-supported nickel catalysts for methane synthesis from pure syngas and syngas containing small amounts of sulfur. A combination of SSITKA and operando FTIR is indicative of both reversible molecular and irreversible dissociative carbon monoxide adsorption on nickel nanoparticles under the reaction conditions. Methanation reaction involves irreversible carbon monoxide adsorption, dissociation, and hydrogenation on nanoparticle steps and edges. Hydrogenation of adsorbed carbon species leading to methane seems to be the reaction kinetically relevant step. Molecular forms of carbon monoxide reversibly adsorbed on nickel terraces are likely not to be involved in carbon monoxide hydrogenation. The results suggest a competition between sulfur and carbon monoxide for nickel surface sites. During methanation, sulfur preferentially adsorbs on the sites of reversible molecular carbon monoxide adsorption, whereas the low-coordinated nickel sites responsible for carbon monoxide dissociation and hydrogenation are affected to a lesser extent by sulfur poisoning. The active sites of carbon monoxide hydrogenation are poisoned much more rapidly by sulfur, when the catalyst has been exposed to small amounts of H_2S in the absence of methanation.

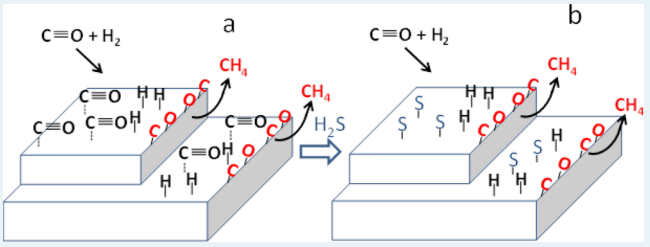

KEYWORDS: *methanation, nickel, deactivation, structure sensitivity, SSITKA, sulfur*

Identification of surface active sites and better understanding of catalyst deactivation are major challenges in nanocatalysis. The geometry of the metal surface site usually has a strong influence on its reactivity, whereas deactivation can spectacularly modify the structure of metal nanoparticles, reduce catalyst lifetime and yield of reaction products. A growing number of investigations have addressed catalyst deactivation.[1−9] Those works involve surface science studies with single crystals and model supported catalysts, in-depth operando characterization under reaction conditions, and ab initio modeling.

Carbon monoxide hydrogenation on metal catalysts leads to methane, higher hydrocarbons, alcohols and other chemicals.[10−15] The reaction occurs on surface sites, which are located on the surface of metal particles (e.g., Ni, Co, Fe, Ru, and Rh) of several nanometers. Syngas for carbon monoxide hydrogenation can be obtained from both fossil and renewable sources (e.g., natural, shale gas, coal, biomass). This makes this reaction particularly suitable for production of alternative ultraclean liquid and gaseous fuels (Fischer−Tropsch diesel, substitute natural gas (SNG), etc.). The methanation reaction[14,15] ($CO + 3H_2 = CH_4 + H_2O$) on nickel catalysts is thermodynamically favorable at low temperatures (<400 °C) but might be limited by kinetics. Information about the catalyst active nanophases, reaction mechanisms, and kinetics is therefore indispensable for optimization of methane production.

The mechanisms and kinetics of methanation on nickel catalysts have been a subject of numerous reports. Structure sensitivity of methanation on nickel catalysts in terms of Boudart[16] has been under debate for a long time. Goodman et al.,[17,18] using single crystal experiments and supported nickels catalysts, concluded that methanation proceeded with similar rates on different nickel surfaces and thus could be a structure insensitive reaction. Nakano et al.[19−21] and Lauritsen et al.[22] observed carbon monoxide dissociation and rapid formation of carbidic species exclusively on stepped Ni surfaces using scanning tunneling microscopy (STM). Recently conducted DFT calculations and ultrahigh vacuum experiments on well-defined single crystals performed by Andersson et al.[23] suggest structure sensitivity of the methanation reaction. In particular, over nickel nanoparticles, the rate of direct carbon monoxide dissociation seems to be much higher on low coordinated sites (e.g., Ni(111) surface steps), whereas no direct carbon

Received: April 2, 2014
Revised: July 11, 2014
Published: July 11, 2014

   dx.doi.org/10.1021/cs500436f | ACS Catal. 2014, 4, 2785−2791

monoxide dissociation was observed over closely packed Ni atoms on the terraces.

Sulfur is one of the major impurities in syngas and a severe poison for metal supported catalysts. Even at residual concentrations of ppm level obtained after gas treatment, sulfur could irreversibly affect the catalytic activity.[24] A single sulfur atom can poison several active sites.[25] Localization of sulfur in nickel nanoparticles and sulfur impact on carbon monoxide hydrogenation kinetics and catalyst deactivation is of utmost importance for optimization of the reaction yield and design of efficient and stable catalysts for carbon monoxide hydrogenation.

The steady-state isotopic transient kinetic analysis (SSITKA) is a powerful technique for investigation of elementary steps and intermediates of catalytic reaction and has been previously successfully used by several research groups.[26−34] The principles of SSITKA have been reviewed by Shannon and Goodwin.[26] In particular, SSITKA addresses[26,27] measuring the transient response of isotopic labels in the reactor following an abrupt change (switch) in the isotopic composition of one of the reactants. The switch involves only isotopic composition of the feed while chemical composition remains unchanged. SSITKA yields crucial information about the concentration of surface intermediates and their residence time without perturbing the steady-state conditions of the catalyst and reactor. A combination of SSITKA with operando FTIR spectroscopy allows time-resolved identification of carbon monoxide molecules adsorbed on the catalyst surface and yields information about their reactivity. Recently, SSITKA employed by groups[29] of Holmen and de Jong has provided important insights into the origin of cobalt particle size effect in Fischer−Tropsch synthesis.

In this study, SSITKA and operando FTIR spectroscopy along with other characterization techniques were used to investigate the influence of small amounts of sulfur in syngas on the elementary steps and kinetics of carbon monoxide hydrogenation and deactivation mechanisms of alumina-supported nickel catalysts.

EXPERIMENTAL SECTION

Ni/γ-Al_2O_3 catalyst (9.5 wt % Ni) was prepared by incipient wetness impregnation of $Ni(NO_3)2.6H_2O$ on SCCA Puralox (SASOL). The catalyst was dried for 3 h at 120 °C and calcined at 500 °C for 5h. The calcined catalyst (30 mg in fixed-bed, 10 mg in IR-cell) was then in situ reduced in pure H_2 flow of 8 sccm/min for 16 h at 400 °C with a 5 °C/min heating rate, followed by cooling at ambient temperature. The reducibility of the catalysts was studied by temperature-programmed reduction (TPR) using an AutoChem II 2920 apparatus (Micromeritics) with a 5 vol % H_2/Ar gas mixture. X-ray powder diffraction experiments were conducted using a Bruker AXS D8 diffractometer using Cu Kα radiation. Surface analyses were performed using a VG ESCALAB 220XL X-ray photoelectron spectrometer (XPS). The catalyst sample after test was transferred to the XPS analysis chamber without any exposure to air.

Carbon monoxide hydrogenation was performed at atmospheric pressure and 250−300 °C. The FTIR spectra were measured using a Nicolet 6700 spectrometer. The carbon monoxide hydrogenation tests were conducted under atmospheric pressure in a millimetric fixed bed reactor (d_{int} = 1.4 mm) with a plug-flow hydrodynamics using a syngas with a H_2/CO stoichiometric ratio of 3 diluted in helium (4He/1CO/3H_2/0.5Ne). The SSITKA apparatus is composed of two independent feed lines. The first line is dedicated to unlabeled compounds and tracer (CO, H_2, He, and Ne), the second one to the isotopic compounds (^{13}CO). Pressure transducers are used to adjust the same pressure drop for both lines. Isotopic switches were realized using a two-position four-way Valco valve and monitored with a QMG 432 Omnistar mass spectrometer in the Faraday mode. To elucidate the modification of the reaction kinetics during carbon monoxide hydrogenation in the absence and in the presence of small amounts of sulfur, SSITKA experiments ($^{12}CO/H_2/He/Ne \rightarrow {}^{13}CO/H_2/He$) were carried out at different times on stream. During catalyst exposure to sulfur-free syngas, the catalytic tests and isotopic switches were performed in the same SSITKA setup. To investigate the effect of sulfur, the catalyst was first exposed to sulfur-containing syngas in a special designed setup built using SulfInert (Restek) tubing and fittings. The setup is equipped with a sulfur sensitive PFPD detector which was used to measure sulfur content upstream and downstream of the catalyst bed. After exposure to syngas with sulfur, the catalyst was transferred without any contact with air to the SSITKA setup for isotopic transient experiments. The catalyst exposure time to sulfur-containing syngas varied from 0 to 60 h. GC analysis were performed with a Shimadzu 2040 equipped with a CP-PoraPLOT and a CTR-1 columns, FID and TCD detectors, which were able to analyze CO_2, CO, and C_1−C_7 hydrocarbons.

RESULTS AND DISCUSSION

The performance of Ni/γ-Al_2O_3 catalyst in carbon monoxide hydrogenation was evaluated using both sulfur-free syngas and syngas containing small amounts of H_2S (H_2S content = 7.5 ppm_v). Conversion of syngas on nickel catalysts under these conditions leads to methane and water (Figure S1, Supporting Information (SI)). Carbon dioxide was observed at higher carbon monoxide conversions and higher reaction temperatures (Figure S1b, SI). In agreement with previous reports,[35,36] the carbon monoxide conversion was quasi stable at relatively low temperatures using sulfur-free syngas (Figure S1a, SI). The drop in catalytic activity was noticeable at higher temperatures (≈300 °C). At 250 °C and GHSV = 18 000 $cm^3\ h^{-1}\ g^{-1}$, carbon monoxide conversion slowly decreases with time on stream from 15.5% corresponding to a 3.6 μmol $g^{-1}\ s^{-1}$ rate to 13.8% after 86 h on stream (3.19 μmol $g^{-1}\ s^{-1}$). These conditions were chosen for conducting SSITKA experiments. It is known that at higher level, water can to some extent inhibit carbon monoxide hydrogenation on nickel catalysts. However, at carbon monoxide conversion of 10−15%, the water effect is expected to be insignificant.[37] To accelerate the catalyst long-term deactivation, the catalyst was also exposed to 300 °C for short periods of time with subsequent returns to 250 °C. The catalytic activity was significantly affected by these high temperature excursions (Figure S1a, SI). Catalyst exposure to syngas containing small amounts of H_2S severely affects the catalyst stability at 250 °C. Analysis of the gas downstream of the reactor with sulfur selective PFPD detector uncovered that all sulfur introduced to the reactor was retained by the nickel catalyst. The decrease in reaction rate is almost proportional to the total amount of sulfur adsorbed on the catalyst (Figure 1). In contrast to the tests performed with sulfur-free syngas, the carbon monoxide conversion in the presence of sulfur drops from 16% to 2% during the first hours of reaction conducted at

dx.doi.org/10.1021/cs500436f | ACS Catal. 2014, 4, 2785−2791

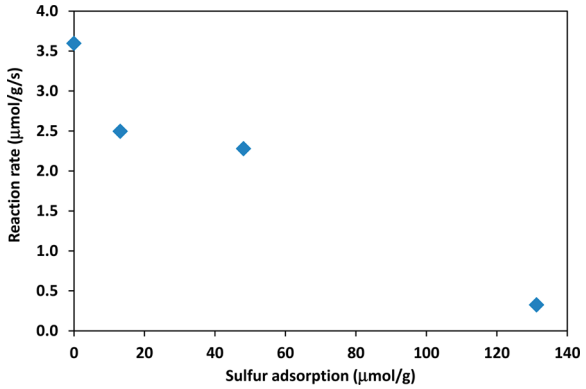

Figure 1. Carbon monoxide hydrogenation rate at 250 °C on Ni/Al_2O_3 catalyst versus amount of adsorbed sulfur (GHSV = 18 000 cm^3 h^{-1} g^{-1}, p = 1 atm, gas composition 4He/1CO/3H_2/0.5Ne).

250 °C, which corresponds to the adsorption of 131 μmol g^{-1} of sulfur on the catalyst.

The reaction intermediates and carbon monoxide reaction pathways were investigated using SSITKA with switches from $^{12}CO/H_2/He/Ne$ to $^{13}CO/H_2/He$. The SSITKA data obtained after the catalyst exposure to sulfur-free syngas after different times on stream are shown in Figure 2a,b. After the switch, a delay is observed between response of inert tracer Ne (τ_{Ne}) and ^{12}CO (τ_{CO}) (Figure 2a). The delay indicates the presence of reversibly adsorbed carbon monoxide molecules on the catalyst surface, which are in equilibrium under the reaction conditions with carbon monoxide in gaseous phase. Interestingly, the delay between Ne and ^{12}CO responses decreases when the catalyst has been exposed to carbon monoxide hydrogenation reaction for a longer time on stream at 250 °C and to higher temperature (300 °C).

The SSITKA experiments suggest a progressive and slow decrease in reversible carbon monoxide adsorption on the catalyst with time on stream. This observation can be due to the decrease in the number of available carbon monoxide adsorption sites (presumably Ni surface atoms) during the reaction. Note that identical experiments performed with the alumina support did not show any delay in the response of carbon monoxide relative to the inert tracer. The amounts of carbon monoxide adsorption sites under the reaction conditions (Figure 3) was estimated from the flow rate of carbon monoxide and transient delay ($\tau_{CO} - \tau_{Ne}$), which represents the average carbon monoxide residence time on the catalyst surface. With sulfur-free gas, the observed decrease in the number of sites of reversibly adsorbed carbon monoxide with the reaction time on stream can be principally due to metal sintering, carbon and gum deposition.[35,36,38−40]

The transient responses of ^{12}C-methane which is a product of carbon monoxide hydrogenation with sulfur-free syngas during switches from $^{12}CO/H_2/He/Ne$ to $^{13}CO/H_2/He$ are also affected by the time on stream and catalyst exposure to 300 °C. Differently to ^{12}CO response, the delay of $^{12}CH4$ response after chromatographic delay subtraction ($\tau_{CH_4} - 0.5\ (\tau_{CO} - \tau_{Ne})$)[29,41] increases (Figure 2b). This suggests an increase in the concentration of chemisorbed intermediates which yield methane through their hydrogenation and desorption (Figure 3a).

Previously, Stockwell[34] and more recently Agnelli et al.[35] suggested that methane formed from the reactive carbide layer which accumulated on the catalyst during carbon monoxide hydrogenation. The presence of the reactive carbon species on the surface of the catalysts exposed to syngas has been further confirmed, in our work by the $^{12}CO/H_2/He/Ne \rightarrow He/Ne \rightarrow {}^{13}CO/H_2/He$ transient experiment (Figure S2, SI). No ^{12}C-methane production was observed after the switch from $^{12}CO/H_2/He/Ne$ to He/Ne for 5 min. The subsequent switch from He/Ne to $^{13}CO/H_2/He$ resulted however in ^{12}C-methane, which was probably produced from ^{12}C reactive carbon species adsorbed on the catalyst surface. The carbon species present on the catalyst surface after carbon monoxide hydrogenation were also characterized using XRD. Figure S3 (SI) displays XRD patterns of the spent catalysts which exhibit the peaks assigned to nickel phases and γ-alumina. A broad small-angle peak characteristic of amorphous phase was observed which was assigned to X-ray scattering over carbon amorphous species accumulated during the reaction.

The adsorbed species present on the catalyst surface during the SSITKA experiments were also characterized by operando FTIR using a specially designed cell (Figure S4, SI). Under of the flow of $^{12}CO/H_2/He/Ne$, the FTIR spectra (Figure 4) were indicative[42−44] of the presence of bridged and linear

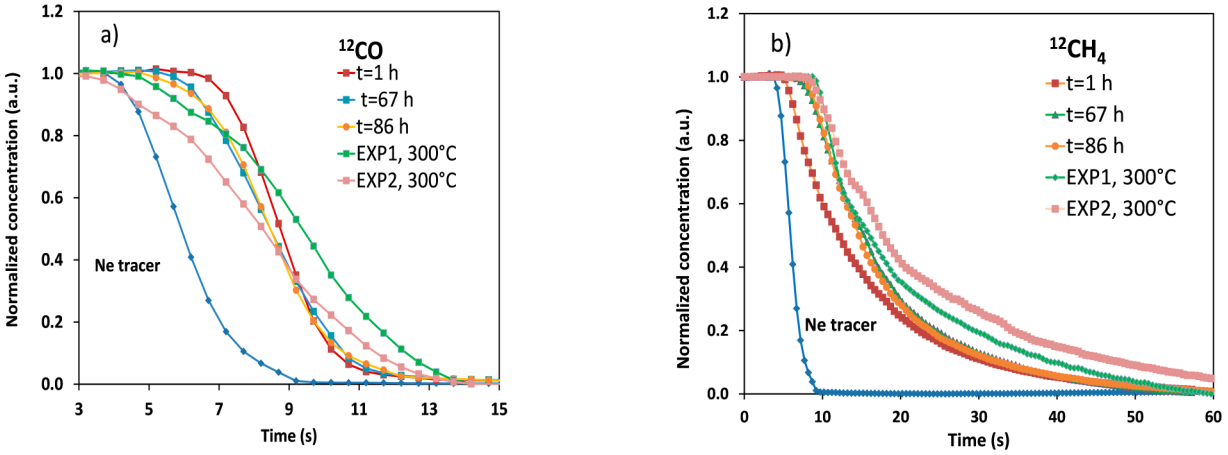

Figure 2. Normalized concentrations of Ne, ^{12}CO (a) and $^{12}CH_4$ (b) during switches $^{12}CO/H_2/Ne \rightarrow {}^{13}CO/H_2$ on the nickel catalyst exposed to sulfur-free syngas with different exposures times (conditions: GHSV = 18 000 cm^3 h^{-1} g^{-1}, p = 1 atm, T = 250 °C, gas composition 4He/1CO/3H_2/0.5Ne).

dx.doi.org/10.1021/cs500436f | ACS Catal. 2014, 4, 2785−2791

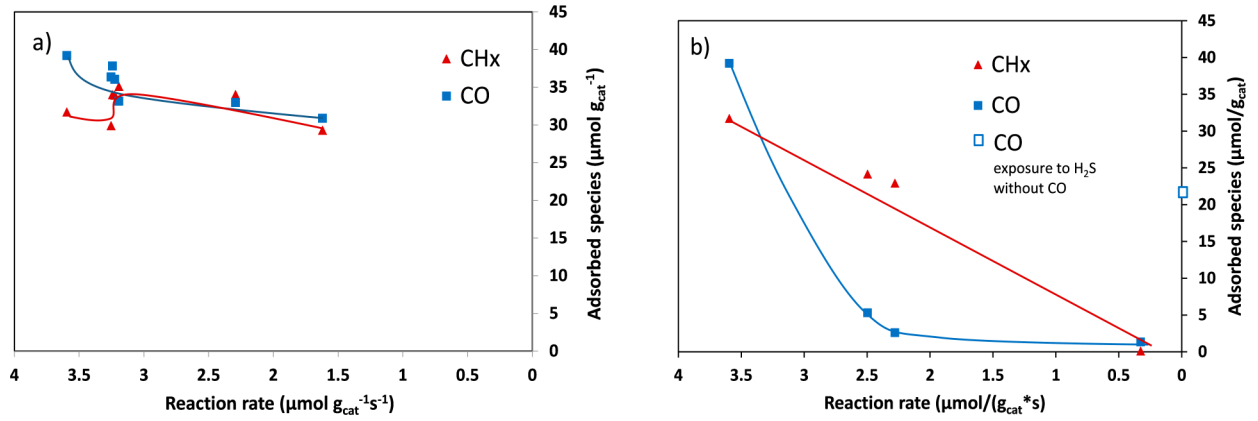

Figure 3. Concentrations of reaction intermediates during carbon monoxide hydrogenation as a function of carbon monoxide reaction rate on nickel catalyst exposed to sulfur-free syngas (a) and to syngas containing 7.5 ppm_v of sulfur (b).

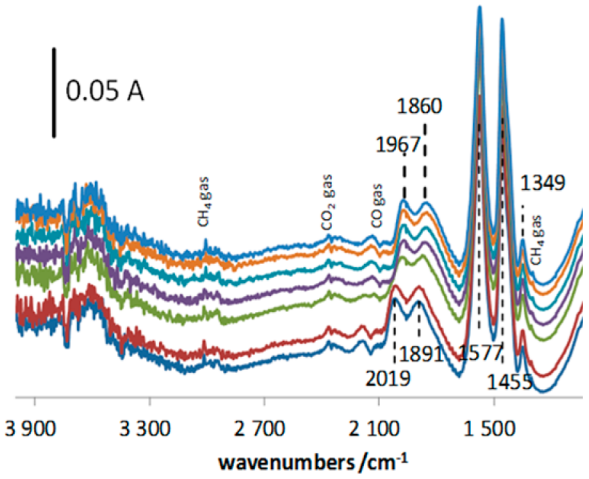

Figure 4. FT-IR spectra of Ni/Al_2O_3 catalyst during $^{12}CO/H_2/Ne \rightarrow {}^{13}CO/H_2$ isotopic switch. The spectra were taken every 1.2 s.

adsorbed carbonyl species characterized by IR bands in $^{12}CO/H_2/He/Ne$ at 2019 and 1891 cm^{-1}, carbonates (possibly monodentates, IR bands at 1577, 1455, and 1349 cm^{-1}).[43,44] Switching from $^{12}CO/H_2/He/Ne$ to $^{13}CO/H_2/He/Ne$ results in a rapid isotopic shift of IR bands assigned to adsorbed carbonyl species, according to square root isotopic ratio of reduced masses (see SI). The characteristic time for $^{12}CO \rightarrow {}^{13}CO$ exchange for the adsorbed carbonyl measured by FTIR (Figure 4) was very similar to the characteristic time for desorption of reversibly adsorbed carbon monoxide species in SSITKA experiments (~5−10 s, Figure S5, SI). This suggests that reversibly adsorbed carbon monoxide species measured from SSITKA experiments correspond to adsorbed carbonyl groups identified using FTIR. Note that the frequency and intensity of IR bands of surface carbonates are not affected by isotopic switch in FTIR. Previous reports[44] suggest that the observed carbonate species are not related to nickel sites and could be located on alumina support. The isotopic switches and operando FTIR data obtained in the present work suggest that these species are not involved in carbon monoxide hydrogenation and can be considered as spectators.

The SSITKA ($^{12}CO/H_2/He/Ne \rightarrow {}^{13}CO/H_2/He$) experiments were also conducted with the catalyst exposed to syngas containing sulfur (7.5 ppm_v, Figure 5). Exposure of the catalyst to even very small amounts of sulfur results in a major decrease in the delay between ^{12}CO response and response of Ne inert tracer (Figure 5a). This drop corresponds to an important decrease in the number of sites of carbon monoxide reversible adsorption on the catalyst. At sulfur adsorption of 13 μmol g^{-1}, CO adsorption drops from 36.7 to 5.3 μmol g^{-1}. Calculations show that catalyst exposure to syngas for 1.5 h corresponds to sulfur adsorption on only 10% of nickel surface sites assuming

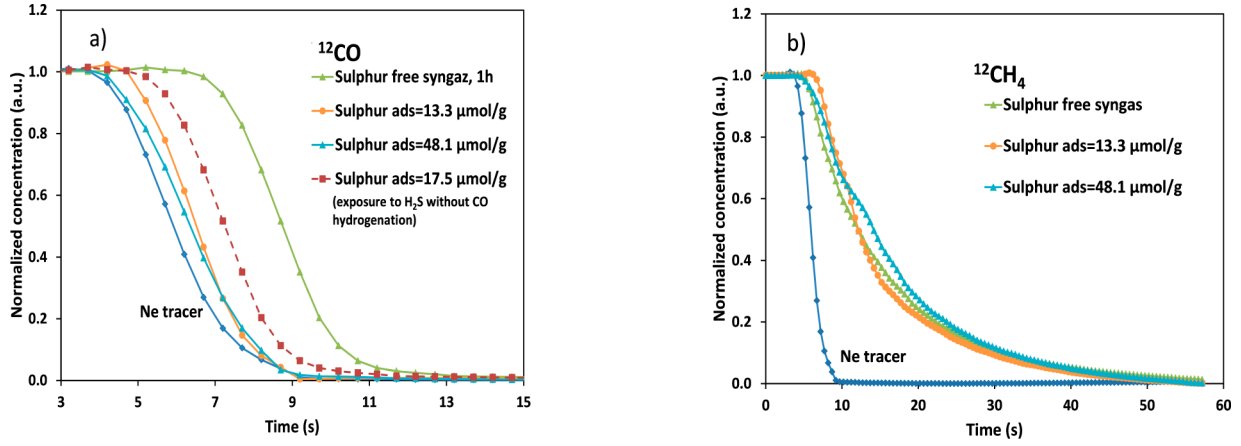

Figure 5. Normalized concentrations of Ne, ^{12}CO (a) and $^{12}CH_4$ (b) during switches of $^{12}CO/H_2/Ne \rightarrow {}^{13}CO/H_2$ on the nickel catalyst exposed to syngas containing 7.5 ppm_v of H_2S (conditions: GHSV = 18 000 cm^3 h^{-1} g^{-1}, p = 1 atm, T = 250 °C, gas composition 4He/1CO/3H_2/0.5Ne).

dx.doi.org/10.1021/cs500436f | ACS Catal. 2014, 4, 2785−2791

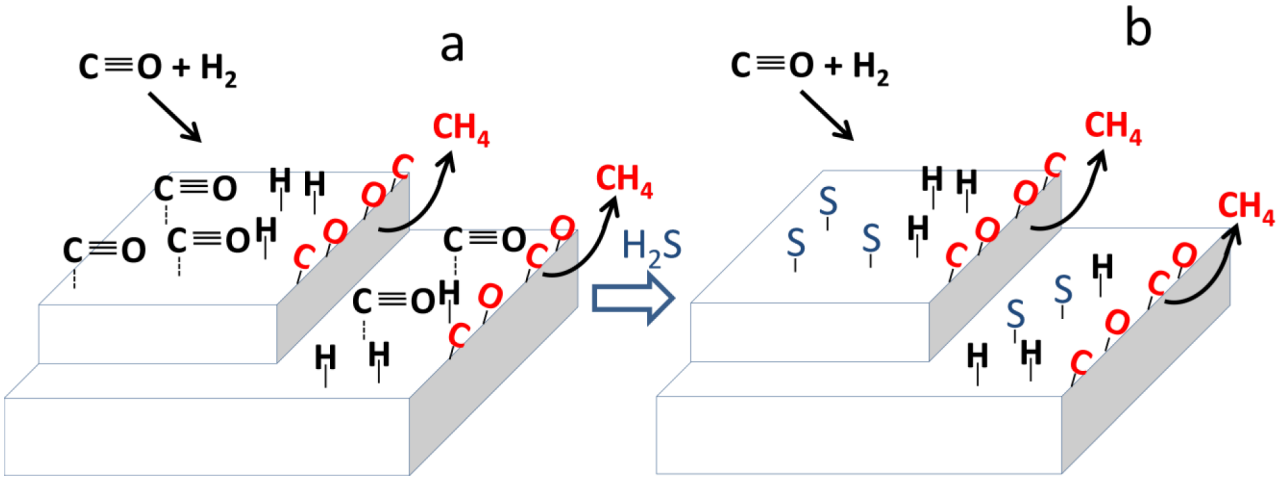

Figure 6. Carbon monoxide hydrogenation with sulfur-free syngas (a) and with syngas containing small amounts of sulfur (b).

the adsorption stoichiometry of 1:1. Interestingly, the number of reversible carbon monoxide adsorption sites decreases much more rapidly than the total number of available Ni surface sites.

Surprisingly, the carbon monoxide hydrogenation rates are affected to a much lesser extent than reversible carbon monoxide adsorption. Catalyst exposure to 13 μmol g^{-1} of sulfur leads to a decrease in carbon monoxide hydrogenation rates only from 3.4 to 2.5 μmol g^{-1} s^{-1} (Figure 1), whereas the number of sites of carbon monoxide reversible adsorption decreases by almost 7−8 times. The $^{12}CH_4$ transient responses are shown in Figure 5b. They are affected to a much lesser extent by exposure to sulfur than those of carbon monoxide. Integration of transient curves suggests that catalyst exposure to sulfur containing gas did not affect to a greater extent the number of reactive carbon intermediates, precursors of methane (Figure 3b). Thus, the formation of reactive carbon species is less affected by sulfur poisoning. Similarly to the catalyst exposed to sulfur-free syngas, XRD characterization of the spent catalysts exposed to sulfur-containing syngas shows the presence of a broad peak presumably attributed to adsorbed amorphous carbon species (Figure S3, SI).

Previously, Stockwell[34] et al. observed adsorbed CO and CH_x species during carbon monoxide hydrogenation on alumina-supported nickel catalysts. The authors suggested that both dissociation of adsorbed CO and CH_x hydrogenation could be kinetically important for this reaction. Sulfur poisoning in our work has provided further insights into the rate-limiting steps of carbon monoxide hydrogenation on nickel catalysts. Catalyst exposure to small amounts of sulfur under the reaction conditions selectively blocks CO adsorption sites, whereas the concentration of CH_x species is only slightly reduced. Thus, the role of adsorbed CO and CH_x intermediates to the overall reaction rate can be clearly evaluated from sulfur poisoning experiments. Interestingly, carbon monoxide hydrogenation rate is not almost affected by selective poisoning of CO adsorption sites (Figure 3b). On the contrary, a linear correlation between carbon monoxide reaction rate and concentration of reactive carbon species was clearly identified from SSITKA data. These reactive carbon intermediates (methane precursors) (Figures 2b and 5b) accumulate under the reaction conditions. Hydrogenation of these species could be the kinetically relevant step of carbon monoxide hydrogenation under the operating conditions. Carbon monoxide adsorption, however, seems not to be a kinetically relevant step even on sulfur pretreated catalysts.

The hypothesis that hydrogenation of reactive carbon species is the rate-limiting step is consistent[37] with the kinetic orders to carbon monoxide and hydrogen (Table S1, SI). Study of the kinetics of methane formation over catalyst exposed to sulfur-free syngas and to syngas with small amounts of sulfur by separate variation of partial pressures of H_2 and CO showed that the reaction order was negative to CO and positive to H_2. These results are in agreement with predicted kinetic orders assuming that hydrogenation of surface carbon species is the reaction rate-limiting step.[37]

Catalyst exposure to H_2S leads to preferential blocking of the sites of reversible carbon monoxide adsorption (which are probably not directly involved in the reaction), whereas the sites responsible for methane production are affected to a much lesser extent by sulfur contamination. The active sites seem to have identical intrinsic activity. Indeed, turnover frequency (TOF) calculations from SSITKA[26] assuming a pseudo-first order reaction with surface carbon hydrogenation as a rate-limiting step show quasi stability during catalyst deactivation via sulfur poisoning (TOF = 0.02 s^{-1}).

Earlier studies[17,18,45] tended to demonstrate that methanation on the Ni surface have no structure sensitivity by demonstrating similar reaction rate for Ni (100), Ni (111) single crystals and supported Ni. DFT calculations recently performed by Andersson et al.[23] indicate, however, the presence of different sites in nickel catalysts. CO can dissociate directly (without hydrogen) on Ni steps (111), although direct carbon monoxide dissociation is rather difficult on Ni terraces (100). The authors attributed the activity in CO methanation to step/edge sites on nickel nanoparticles (Figure 6a). Our results suggest that sulfur could principally block the sites of reversible molecular carbon monoxide adsorption possibly on Ni (100) terraces (Figure 6b). XPS of the catalyst exposed to carbon monoxide hydrogenation in the presence of small amounts of sulfur (Figure S6, SI) showed the presence of sulfide species on the catalyst surface. Several Ni sites can be blocked by a single adsorbed sulfur atom. Carbon monoxide hydrogenation activity seems to be related to Ni atoms on steps where carbon monoxide dissociation proceeds rather fast. To confirm this suggestion, the ease of carbon monoxide dissociation on the nickel catalyst was checked in this work by exposure of a catalyst after carbon monoxide hydrogenation

dx.doi.org/10.1021/cs500436f | ACS Catal. 2014, 4, 2785−2791

catalytic test (>10h) to pure carbon monoxide at 250 °C. Very rapid production of carbon dioxide which is due to carbon monoxide disproportionation: $2CO{=}C+CO_2$ was clearly observed (Figure S7, SI).

To figure out whether carbon species produced during carbon monoxide hydrogenation can protect to some extent the active sites for sulfur poisoning, nickel catalyst was exposed to 7.5 ppm_v of H_2S without CO in inlet gas composition. Carbon monoxide was replaced by nitrogen in the gas feed. The catalyst pretreated with H_2S without syngas did not show any carbon monoxide conversion under the reaction conditions. At the same time, SSITKA showed clearly reversible adsorption of CO on this sample (Figures 3b and 5a). In the absence of carbon monoxide hydrogenation, catalyst exposure to small amounts of H_2S results in sulfur poisoning of the CO dissociation site (steps and edges). During the carbon monoxide hydrogenation, because of competition with carbon species, sulfur adsorption primarily occurred on molecular CO adsorption sites (terraces). In this case sulfur adsorption on Ni steps seems to be hindered by a layer of reactive carbon. Adsorbed carbon species seems to protect to some extent nickel catalysts from sulfur poisoning. Consequently, the catalyst stability is 10 times higher if sulfur deposition occurs during methanation reaction compared to sulfur deposition on the catalyst without methanation.

CONCLUSION

A combination of SSITKA with operando FTIR and other characterization techniques uncovered the presence of several adsorbed carbon species in working nickel methanation catalysts: carbonate groups presumably located on alumina support, molecular forms of adsorbed CO, reactive carbon species produced via carbon monoxide dissociation. Carbonates and molecular forms of adsorbed CO are probably spectators in carbon monoxide hydrogenation. The reaction proceeds via very fast direct carbon monoxide dissociation leading to the formation of adsorbed reactive carbon species. Hydrogenation of reactive carbon species seems to be the rate-limiting step in CO methanation. Under the methanation conditions, sulfur atoms preferentially adsorb on the sites of reversible molecular carbon monoxide adsorption. The sites responsible for carbon monoxide dissociation, which leads to methane production, are affected to a lesser extent by sulfur poisoning. In the absence of carbon monoxide hydrogenation, sulfur preferentially blocks the sites of irreversible carbon monoxide which lead to more rapid catalyst deactivation.

This work yields new fundamental information about active sites and deactivation phenomena in supported nickel catalysts for carbon monoxide hydrogenation. In addition, the developed methodology is applicable for other catalytic reactions and can also provide major insights into the evolution of their structure and intrinsic activity.

ASSOCIATED CONTENT

Supporting Information

Steady-state carbon monoxide hydrogenation data, XRD patterns, TPR profiles, XPS data, schema of operando FTIR cell, transient data showing fast carbon monoxide disproportionation on nickel catalyst, results of combined SSITKA-MS-IR experiment, kinetic orders, detail of nickel metal sites estimation. This material is available free of charge via the Internet at http://pubs.acs.org.

AUTHOR INFORMATION

Corresponding Author

*E-mail: andrei.khodakov@univ-lille1.fr. Fax: +33 3 20 43 65 61. Tel.:+33 3 20 33 54 39.

Author Contributions

The manuscript was written through contributions of all authors. All authors have given approval to the final version of the manuscript.

Notes

The authors declare no competing financial interest.

ACKNOWLEDGMENTS

The authors gratefully acknowledge financial support for this work from the French National Agency for Research (Biosyngop Project, no. ANR-11-BS07-026).

REFERENCES

(1) Li, Y.; Hung-Chang Liu, J.; Witham, C. A.; Huang, W.; Marcus, M. A.; Fakra, S. C.; Alayoglu, P.; Zhu, Z.; Thompson, C. M.; Arjun, A.; Lee, K.; Gross, E.; Toste, F. D.; Somorjai, G. A. *J. Am. Chem. Soc.* **2011**, *133*, 13527−13533.

(2) Bartholomew, C. H. *Appl. Catal., A* **2001**, *212*, 17−60.

(3) Parvulescu, A. N.; Mores, D.; Stavitski, E.; Teodorescu, C. M.; Bruijnincx, P. C. A.; Gebbink, R. J. M. K.; Weckhuysen, B. M. *J. Am. Chem. Soc.* **2010**, *132*, 10429−10439.

(4) Govind Menon, P. *Chem. Rev.* **1994**, *94*, 1021−1046.

(5) Saib, A. M.; Moodley, D. J.; Ciobîcă, I. M.; Hauman, M. M.; Sigwebela, B. H.; Weststrate, C. J.; Niemantsverdriet, J. W.; van de Loosdrecht, J. *Catal. Today* **2010**, *154*, 271−282.

(6) Tsakoumis, N. E.; Rønning, M.; Borg, Ø.; Rytter, E.; Holmen, A. *Catal. Today* **2010**, *154*, 162−182.

(7) Challa, S. R.; Delariva, A. T.; Hansen, T. W.; Helveg, S.; Sehested, J.; Hansen, P. L.; Garzon, F.; Datye, A. K. *J. Am. Chem. Soc.* **2011**, *133*, 20672−20675.

(8) Mattos, L. V.; Jacobs, G.; Davis, B. H.; Noronha, F. B. *Chem. Rev.* **2012**, *112*, 4094−4123.

(9) Moulijn, J. A.; van Diepen, A. E.; Kapteijn, F. *Appl. Catal., A* **2001**, *212*, 3−16.

(10) Iglesia, E. *Appl. Catal.* **1997**, *161*, 59−78.

(11) Dry, M. *Catal. Today* **2002**, *71*, 227−241.

(12) Van Steen, E.; Clayes, M. *Chem. Eng. Technol.* **2008**, *31*, 655−666.

(13) Khodakov, A. Y.; Chu, W.; Fongarland, P. *Chem. Rev.* **2007**, *107*, 1692−1744.

(14) Kopyscinski, J.; Schildhauer, T. J.; Biollaz, S. M. A. *Fuel* **2010**, *89*, 1763−1783.

(15) Huber, G. W.; Iborra, S.; Corma, A. *Chem. Rev.* **2006**, *106*, 4044−4098.

(16) Boudart, M. *Chem. Rev.* **1995**, *95*, 661−666.

(17) Goodman, G. M.; Kelley, R. D.; Madey, T. E.; Yates, J. T. J. *J. Catal.* **1980**, *63*, 226−234.

(18) Goodman, D. W. *Acc. Chem. Res.* **1984**, *17*, 194−200.

(19) Nakano, H.; Kawakami, S.; Fujitani, T.; Nakamura, J. *Surf. Sci.* **2000**, *454*, 295−299.

(20) Nakano, H.; Nakamura, J. *Surf. Sci.* **2001**, *482*, 341−345.

(21) Nakano, H.; Ogawa, J.; Nakamura, J. *Surf. Sci.* **2002**, *514*, 256−260.

(22) Lauritsen, J. V.; Vang, R. T.; Besenbacher, F. *Catal. Today* **2006**, *111*, 34−43.

(23) Andersson, M. P.; Abild-Pedersen, F.; Remediakis, I. N.; Bligaard, T.; Jones, G.; Engbæk, J.; Lytken, O.; Horch, S.; Nielsen, J. H.; Sehested, J.; Rostrup-Nielsen, J. R.; Nørskov, J. K.; Chorkendorff, I. *J. Catal.* **2008**, *255*, 6−19.

(24) Struis, R. P. W. J.; Schildhauer, T. J.; Czekaj, I.; Janousch, M.; Biollaz, S. M. A.; Ludwig, C. *Appl. Catal., A* **2009**, *362*, 121−128.

(25) Goodman, D. W.; Kisiunova, M. *Surf. Sci.* **1981**, *105*, L265−L270.
(26) Shannon, S. L.; Goodwin, J. G. *Chem. Rev.* **1995**, *95*, 677−695.
(27) Efstathiou, A. M.; Gleaves, J. T.; Yablonsky, G. S. *Characterization of Solid Materials and Heterogeneous Catalysts: From Structure to Surface Reactivity*; Che, M., Vedrine, J. C., Eds.; Wiley-VCH Verlag GmbH: Weinheim, Germany, 2012; pp 1013−1073
(28) Schweicher, J.; Bundhoo, A.; Frennet, A.; Kruse, N.; Daly, H.; Meunier, F. C. *J. Phys. Chem. C* **2010**, *114*, 2248−2255.
(29) den Breejen, J. P.; Radstake, P. B.; Bezemer, G. L.; Bitter, J. H.; Frøseth, V.; Holmen, A.; de Jong, K. P. *J. Am. Chem. Soc.* **2009**, *131*, 7197−7203.
(30) van Dijk, H. A. J.; Hoebink, J. H. B. J.; Schouten, J. C. *Chem. Eng. Sci.* **2011**, *56*, 1211−1219.
(31) Kalamaras, C. M.; Dionysiou, D. D.; Efstathiou, A. M. *ACS Catal.* **2012**, *2*, 2729−2742.
(32) El-Roz, M.; Bazin, P.; Daturi, M.; Thibault-Starzyk, F. *ACS Catal.* **2013**, *3*, 2790−2798.
(33) Kalamaras, C. M.; Gonzalez, I. D.; Navarro, R. M.; José Luis, G.; Fierro, J. L. G.; Efstathiou, A. M. *J. Phys.Chem. C* **2011**, *115*, 11595−11610.
(34) Stockwell, D. M.; Chung, J. S.; Bennett, C. O. *J. Catal.* **1988**, *112*, 135−144.
(35) Agnelli, M.; Swaan, H. M.; Marquez-Alvarez, C.; Martin, G. A.; Mirodatos, C. *J. Catal.* **2008**, *175*, 117−128.
(36) Parlikkad, N. R.; Chambrey, S.; Fongarland, P.; Fatah, N.; Khodakov, A.; Capela, S.; Guerrini, O. *Fuel* **2013**, *107*, 254−260.
(37) Sughrue, E. L.; Bartholomew, C. H. *Appl. Catal.* **1982**, *2*, 239−256.
(38) Mirodatos, C.; Praliaud, H.; Primet, M. *J. Catal.* **1987**, *107*, 275−287.
(39) Rostrup-Nielsen, J. R.; Pedersen, K.; Sehested, J. *Appl. Catal., A* **2007**, *330*, 134−138.
(40) Bartholomew, C. H. *Catal. Rev.* **1982**, *24*, 67−112.
(41) Biloen, P.; Helle, J. N.; van den Berg, F. G. A.; Sachtler, W. M. H. *J. Catal.* **1983**, *81*, 450−463.
(42) Rewick, R. T.; Wise, H. *J. Phys. Chem.* **1978**, *82*, 751−752.
(43) Iordan, A.; Zaki, M. I.; Kappenstein, C. *Phys. Chem. Chem. Phys.* **2004**, *6*, 2502−2512.
(44) Sanchez-Escribano, V.; Larrubia Vargas, M. A.; Finocchio, E.; Busca, G. *Appl. Catal., A* **2007**, *316*, 68−74.
(45) Rostrup-Nielsen, J. R.; Pedersen, K. *J. Catal.* **1979**, *59*, 395−404.